Rev. Adv. Mater. Sci. 57 (2018) 143-150

MODELING C_{540}-C_{20} FULLERENE COLLISIONS

Leysan Kh. Rysaeva[1], Ivan P. Lobzenko[2], Julia A. Baimova[1,3], Sergey V. Dmitriev[1,4] and Kun Zhou[5]

[1]Institute for Metals Superplasticity Problems of the Russian Academy of Sciences, Khalturina 39, Ufa 450001, Russia
[2]Institute of Molecule and Crystal Physics - Subdivision of the Ufa Federal Research Centre of the Russian Academy of Sciences, Pr. Oktyabrya 151, Ufa 450075, Russia
[3]Bashkir State University, Validy Str. 32, Ufa 450076, Russia
[4]National Research Tomsk State University, Lenin Ave, 36, 634050 Tomsk, Russia
[5]School of Mechanical and Aerospace Engineering, Nanyang Technological University, 50 Nanyang Avenue, Singapore 639798, Singapore

Received: May 22, 2018

Abstract. Collisions of C_{20} and C_{540} fullerenes are studied in a wide range of velocities by means of classical molecular dynamics. The simulations show that the collision scenario strongly depends on the collision velocity of the fullerenes. At low collision energies, the fullerenes are repelled by the van der Waals forces, and after bouncing off a part of the kinetic energy of their translational motion is converted into the energy of cage vibrations. At higher collision energies, the fullerenes overcome the potential barrier of Pauli repulsion with the formation of the new chemical bonds, and a significant change in the geometry of the molecules is observed. At very high collision energies, structure of the molecules is destroyed with the formation of new carbon clusters. Analysis of collisions for fullerenes of significantly different size revealed some new features associated with their asymmetric energy exchange.

1. INTRODUCTION

The discovery of fullerenes in 1985 has opened era of carbon nano-polymorphs [1]. Fullerene molecules of different sizes possess various unique properties which opens wide possibilities of their application for fuel [2] and solar [3] cells, in biomedicine [4,5], for synthesis of fullerene reinforced composites [6,7], for designing nano-devices [8], to name a few. The possibility of application of fullerenes as the hydrogen storage cells is also considered [9-11]. It is shown that especially giant fullerenes (C_{720}) can contain more than 6.5 wt.% of hydrogen atoms [9]. The great interest in the investigation of fullerene molecules is connected with their high structural stability, symmetry [12], variety of shapes and non-negative Gaussian curvature everywhere [12]. Fullerene outer surface is available for chemical modification, while its inner space is available for the encapsulation of a variety of chemical elements [13]. Moreover, fullerenes are the base elements for such solid structures as fullerite [14], diamond-like phases [15-21] and they undergo phase transition to polycrystalline diamond at the pressure higher than 20 GPa [22].

It is well-known that fullerene family contains several molecules ranging from C_{20} to C_{960} [23-26]. The most abundant fullerenes are C_{60} and C_{70} which can be synthesized by evaporation of carbon, incomplete combustion of benzene in oxygen and microwave method [27-28]. Coalescence of fullerenes into large fullerenes up to C_{300} has been observed in the gas phase and inside carbon nanotubes [29,30]. Collision-induced fusion of fullerenes has been characterized by means of first-

Corresponding author: I.P. Lobzenko, e-mail: ivan.lobzenko@gmail.com

principle molecular dynamics simulations and it has been shown that the highest probability of fusion is observed for collision energies of 120-140 eV [31]. However, it is interesting to note that fullerene formation mechanisms are still largely unknown. Study of the interaction and collision between different fullerene molecules is of significant interest. A wealth of experiments and numerical calculations devoted to fullerenes collisions have been performed in the past years [32-34] including electron capture and ionization of C_{60} [35]; fusion and fragmentation of C_{60} induced by ion impact [36,37] or collisions with surfaces [38]; fusion, fragmentation and charge transfer induced by fullerene collisions [39-42]. After the pioneering C^{+}_{60} C_{60} collision experiment [39], cluster-cluster collisions became a versatile new field of research. Collisions between highly charged Xe^{20+} ions and fullerene van der Waals clusters have been found to lead to molecular growth [32]. At the same time, a little attention is given to the collisions of fullerenes of different sizes, for example, the collision of the smallest known fullerene C_{20} and one of the giant fullerenes C_{540}.

Despite the study of fullerene collisions has been going on for more than twenty years, an experimental study of the dynamics of collisions remains difficult, and the results of such experiments often contradict each other [43]. Molecular dynamics (MD) simulation is a robust numerical method to address nanoscale phenomena. MD calculations can reveal the physical and chemical properties of various carbon nano-structures or can help to devise the possible formation pathways. Existing potential functions allow to simulate both covalent bonds between carbon atoms and van der Waals forces between fullerene molecules.

In this study, MD simulations of fullerene collisions are conducted at a temperature close to zero. Collision of the smallest possible fullerene C_{20} and one of the giant fullerenes C_{540} is considered in a wide range of velocities.

2. SIMULATION DETAILS

Fig. 1 illustrates the simulation setup for equilibrium fullerenes C_{540} and C_{20} with the initial distance between their centers of mass equal to 30 Å. At this distance the closest carbon atoms of fullerenes are far from each other and do not interact. The centers of mass of the fullerenes are on the *x*-axis and they move toward each other with the initial velocities V_{C540}=-V_{C20}/27 keeping the center of mass of the whole system at rest, since C_{540} is 27 times heavier than C_{20}. The dimensions of the simulation box are 10000x55x55 Å with the periodic boundary conditions applied along all three directions.

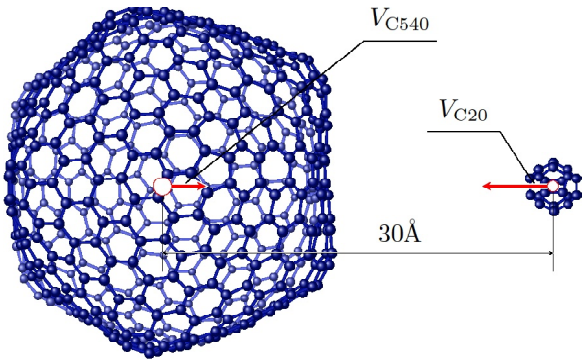

Fig. 1. The initial state: two equilibrium fullerenes C_{540} and C_{20} are the initial distance of 30 Å between their centers of mass moving toward each other with the velocities V_{C540}=-V_{C20}/27 so that the center of mass of the whole system is at rest.

All the simulations are carried out using the LAMMPS platform [44] with the well-known AIREBO potential [45].

The non-bonding interactions between fullerenes are the van der Waals forces, which are attractive, while at smaller distances repulsive Pauli interactions come into play. The most common way to describe the van der Waals interactions gives the Lenard-Jones potential which is already included into AIREBO. Proper definition of interatomic forces is one of the most essential factors in MD modeling. AIREBO potential is the member of classical bond-order family of the Tersoff-Brenner potentials which effectively manipulate covalent bonds in non-polar systems. Previously, AIREBO potential was successfully used for the similar studies, for example, the collision between fullerene and graphene [33], self-assembly of fullerenes and graphene [46], ion collisions with clusters of C_{60} fullerenes [34], growth of fullerenes and nanotubes [47-49], etc.

Equilibrium atomic configurations of fullerenes are found before the collision simulation. The equilibration is conducted at temperature close to 0K and the canonical ensemble (NVT) is employed. A time step of 0.5 fs is taken for the simulation. After the equilibrium positions were found, the initial velocities are introduced along the line connecting fullerenes' centers of mass, which coincides with *x*-axis. For these simulations the NVE ensemble is used. Thermal fluctuations at initial moment are absent. The velocity of the smaller fullerene (V_{C20}) is chosen as a control parameter and collisions are simulated within a broad range of its values, from 1 to 150 Å/ps.

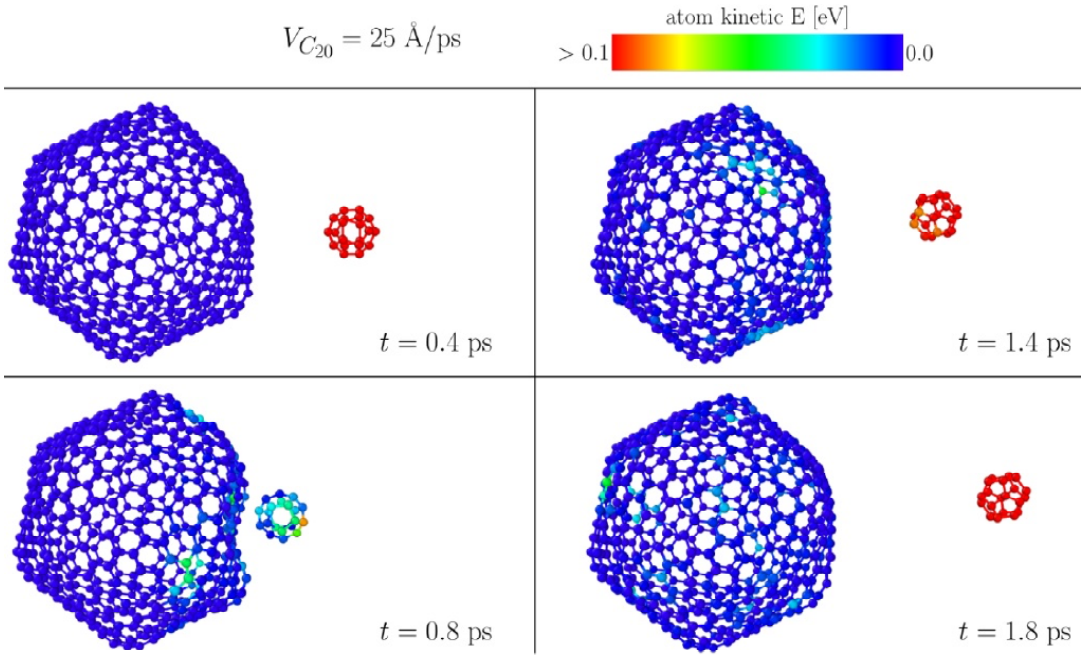

Fig. 2. Snapshots of the fullerene collision at the initial velocity V_{C20}=25 Å/ps. Similar picture is observed for fullerenes colliding at a velocity within the range V_{C20}<83 Å/ps. Atoms are colored in accordance with their kinetic energy

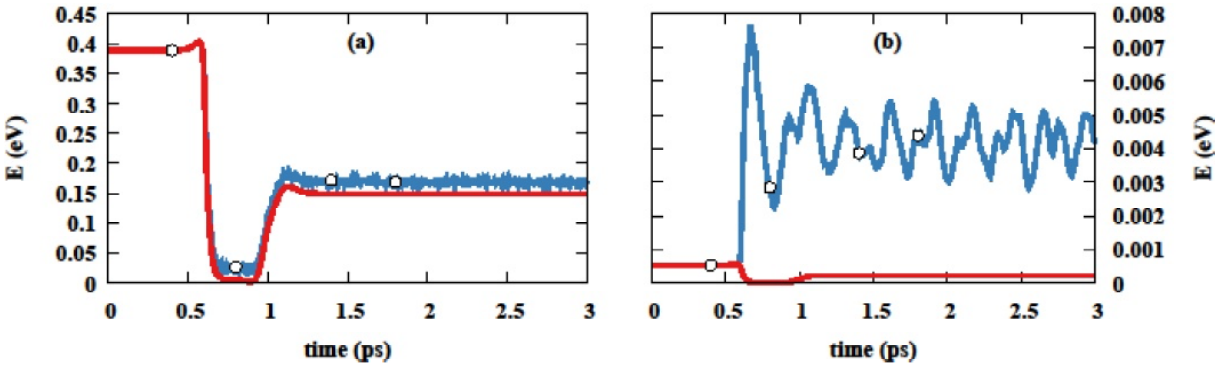

Fig. 3. Kinetic energy per atom (blue curves) and kinetic energy of the center of mass per atom (red curves) for (a) C_{20} and (b) C_{540} colliding at the initial velocity of V_{C20}=25 Å/ps. Open dots on the curves correspond to the snapshots from Fig. 2.

3. RESULTS AND DISCUSSION

The obtained results suggest that the fullerene collisions follow three different regimes depending on the initial velocity V_{C20}.

For the velocity of V_{C20}<87 Å/ps, two fullerenes after collision move away from each other without any recombination of chemical bonds with the absolute velocities less than before the collision, since a part of the kinetic energy of their translational motion is transformed into the energy of cage oscillations. The repulsion of two fullerenes took place because of the Pauli interaction and elasticity of the cages. Typical picture of the fullerene collision at relatively small velocity is presented in Fig. 2 for V_{C20}<25 Å/ps. Here and further, atoms are colored in accordance with their kinetic energy. As it can be seen, at first (Fig. 2a) all the atoms of C_{20} have highest kinetic energy, while C_{540} atoms have much smaller energy due to the large difference in their initial velocities. During the collision, kinetic energy of fullerenes is partly transformed into elastic deformation energy of cages but after the fullerenes bounce off, a part of the elastic energy returns into the energy of translational motion.

In order to quantify the energy flow in the system, in Fig. 3 kinetic energy per atom (blue lines) and kinetic energy of the center of mass per atom (red lines) for (a) C_{20} and (b) C_{540} colliding with the initial velocity V_{C20}=25 Å/ps is plotted. Recall that total energy (kinetic plus potential) is conserved in

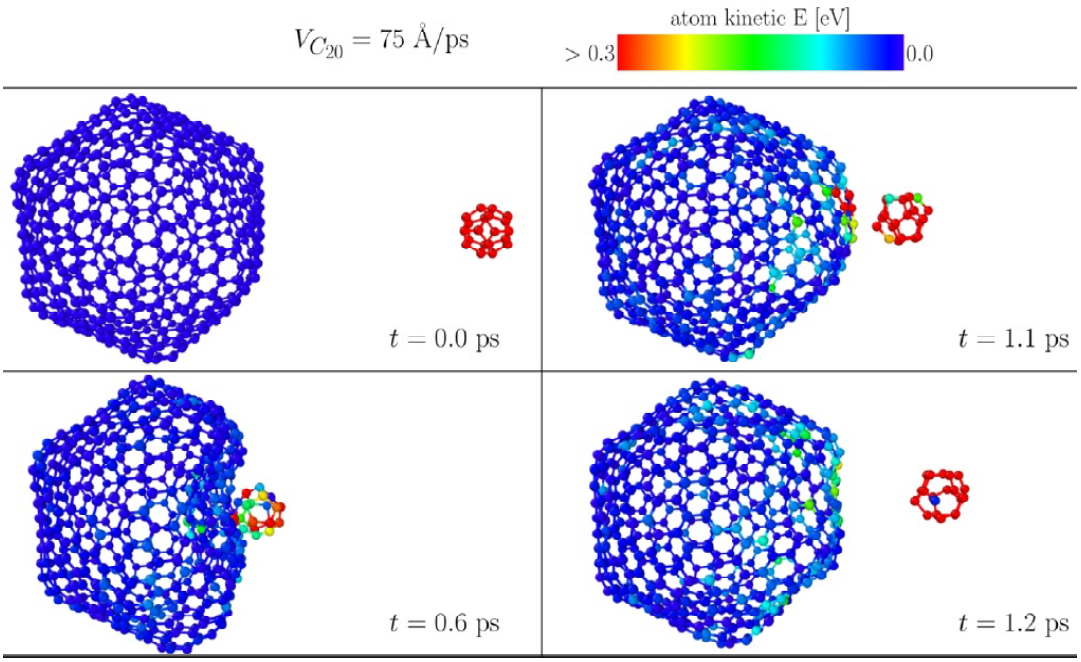

Fig. 4. Snapshots of the fullerene collision at the initial velocity V_{C20}=75 Å/ps. This collision velocity is close to the threshold value V_{C20}=83 Å/ps above which structural changes appear in the cages.

the system. Kinetic energy of the center of mass does not include the kinetic energy related to internal motion of molecules and reflects only their translational motion. Open dots in Fig. 3 correspond to the snapshots from Fig. 2. As it can be seen, for both fullerenes before the collision the kinetic energy is equal to the kinetic energy of the center of mass because internal vibrational modes are not excited. At the moment of collision (t=0.8 ps), the kinetic energy of the system is redistributed due to the excitation of the internal vibrational modes of each fullerene. The collision lasts for approximately 0.3 ps, when the kinetic energy of the fullerenes' centers of mass is close to zero. For the considered collision velocity V_{C20}=25 Å/ps, the kinetic energy of the centers of mass of the fullerenes after collision is less than half the initial value. Within the velocity range V_{C20}<83 Å/ps, the higher V_{C20}, the greater portion of the translational energy of fullerenes goes into their internal vibrations. It should be noted, that the large difference in the fullerene size causes the asymmetry in the energy exchange between them. Most of the translational energy of C_{20} is expended to the heating of C_{540}. Indeed, after the collision, the kinetic energy per atom of C_{540} oscillates at the level of 0.004 eV, while the energy of its translational motion is an order of magnitude smaller. On the other hand, most of the kinetic energy of C_{20} after collision remains in the form of translational energy. This can be explained by the fact that C_{540} fullerene has a larger number of normal vibrational modes, the excitation of which occurs during the collision.

The pre-critical behavior of the fullerenes is shown in Fig. 4 for V_{C20}=75 Å/ps. Atoms are colored in accordance with their kinetic energy. As it can be seen, during the collision, considerable deformation of the giant fullerene takes place, however after the collision its quasi-spherical structure is restored being perturbed by intrinsic oscillations.

For the collision velocity range 83<V_{C20}<140 Å/ps, fullerenes have enough energy to overcome the Pauli repulsion barrier, and formation of new chemical bonds between two fullerenes occurs. The interaction dynamics for representative velocity V_{C20}=85 Å/ps is illustrated in Fig. 5. It should be noted, that the hybridization of the atoms participating in the formation of new bonds changes which leads to the local change in the fullerene geometry. From Fig. 6, where the example of the new covalent bond formation is presented, the appearance of a sharp ledge can be seen. It is found that a lower potential energy of the system can be achieved if one more covalent bond is formed. Under this structural transformation, the appearance of the concave region on C_{540} fullerene is beneficial due to van der Waals forces acting between two molecules.

In Fig. 7 the same as in Fig. 3 but for the collision velocity V_{C20}=85 Å/ps is presented. It can be seen, that even after the collision the kinetic energy of the centers of mass of two bonded fullerenes drops to zero, since the total momentum of the sys-

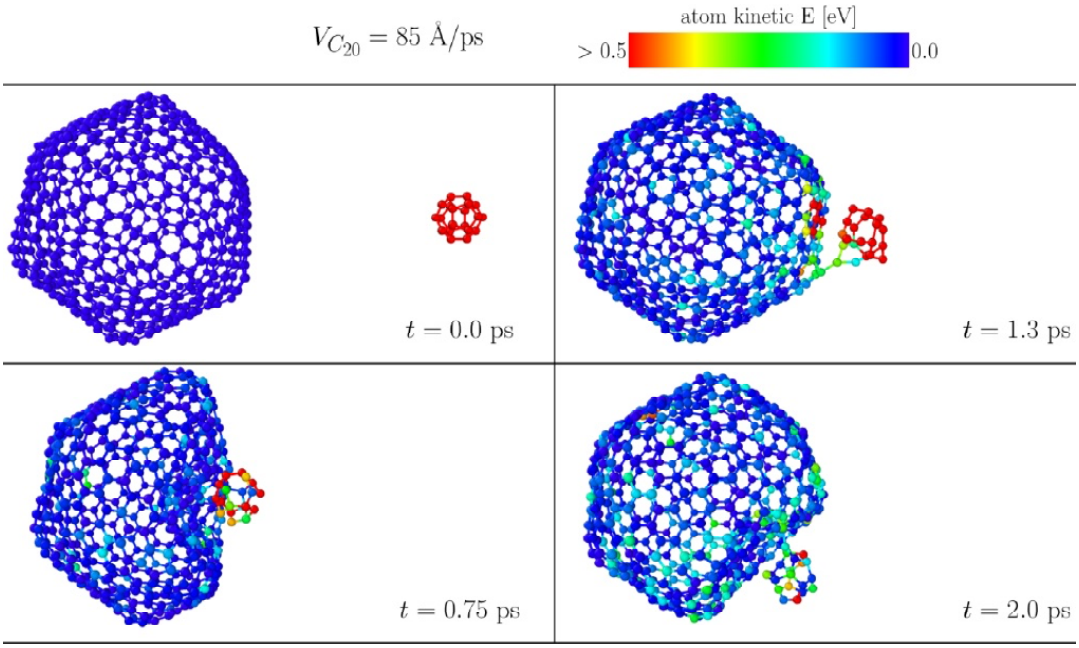

Fig. 5. Snapshots of the fullerene collision at the initial velocity V_{C20}=85 Å/ps. Similar picture is observed for collision velocities in the range 83<V_{C20}<140 Å/ps.

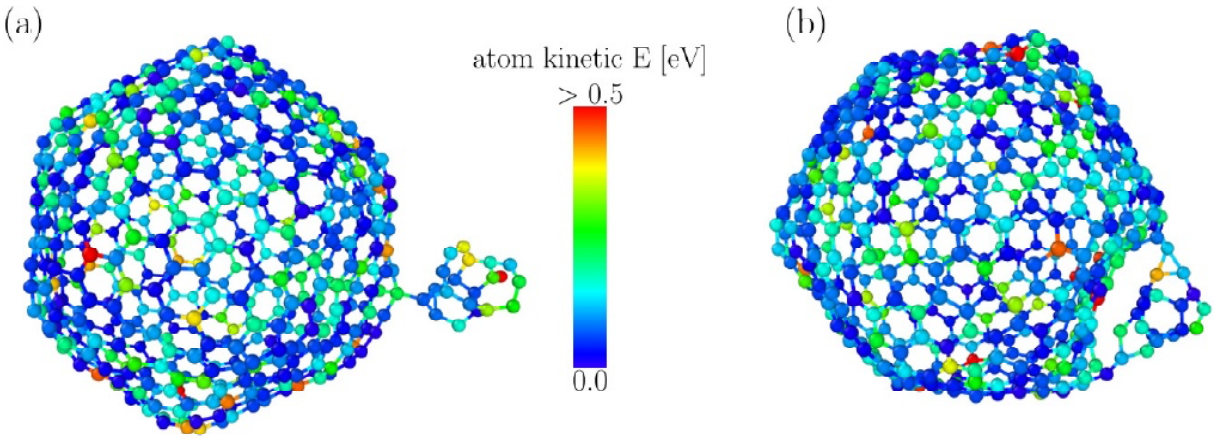

Fig. 6. Snapshots of the fullerene collision for the initial velocity V_{C20}=85 Å/ps. Similar scenario is observed for collision velocities within the range 83<V_{C20}<140 Å/ps. (a) The formation of one new covalent bond and (b) formation of the second covalent bond, which is beneficial due to the strong geometrical transformation of the fullerenes.

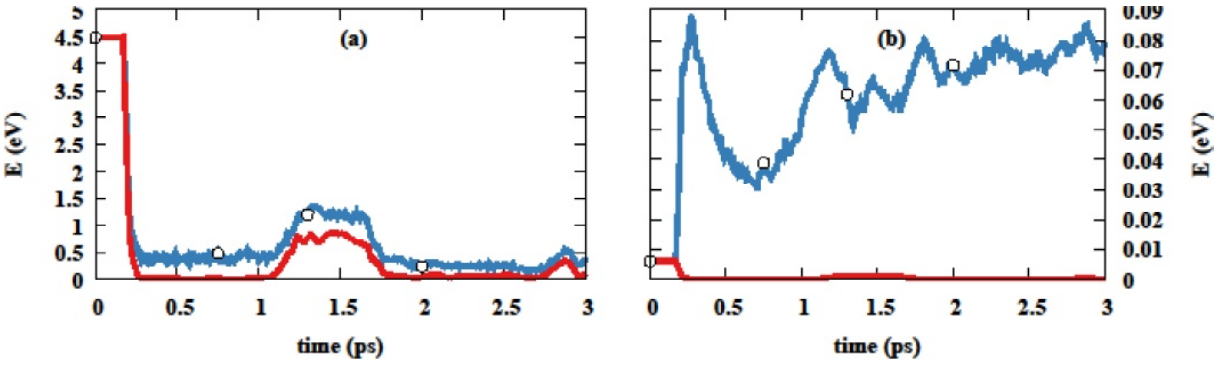

Fig. 7. Same as in Fig. 3 but for V_{C20}=85 Å/ps. Open dots on the curves correspond to the snapshots from Fig. 5.

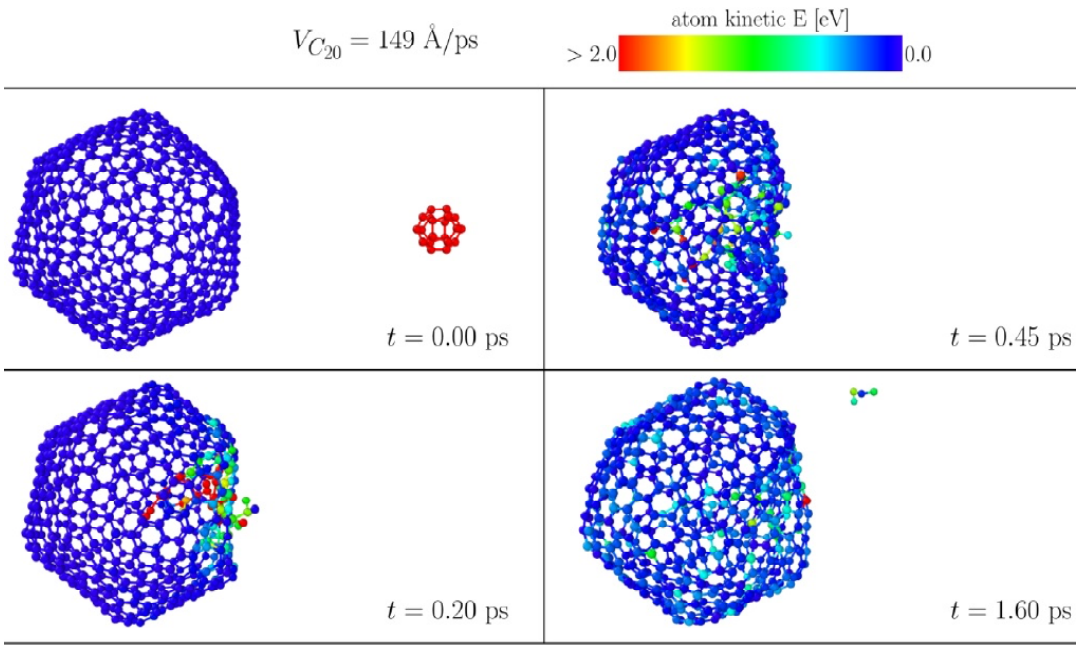

Fig. 8. Snapshots of the fullerene collision at the initial velocity V_{C20}=149 Å/ps. Destruction of the small fullerene takes place with the formation of smaller carbon cluster.

tem is zero. Thus, the entire energy of the translational motion of the fullerenes goes into their internal vibrational modes and for creation of new valence bonds. In Fig. 7, a temporary increase in the kinetic energy of the mass centers of fullerenes is observed for 1.1<*t*<1.8 ps. Within this interval, two molecules connected by a single covalent bond move away after a maximum approach, but being unable to break a newly created bond, they again come together to create the second bond. The molecule merging process takes about 1.5 ps.

For the initial velocity greater than 140 Å/ps another scenario is observed: the collision of two fullerenes causes the destruction of one or both molecules. Example of such dynamics is presented in Fig. 8. As the result of collision C_{20} is destroyed and a cluster of four carbon atoms is separated and moves away.

4. CONCLUSIONS

Collision of a giant fullerene C_{540} with the smallest fullerene C_{20} is investigated by molecular dynamics simulation for various collision velocities. Three main scenarios of fullerene collision are found depending on the collision velocity within the range $0<V_{C20}<150$ Å/ps ($V_{C540}=-V_{C20}/27$).

For relatively slow collisions, $V_{C20}<83$ Å/ps, fullerenes retain initial structure and move apart with the absolute velocities less than initial ones, since a part of their kinetic energy of the translational motion transforms into the energy of internal oscillations. The asymmetry of the energy redistribution, caused by the difference in the sizes of the interacting molecules, leads to the energy of the translational motion of the small fullerene being spent to heat the large one. This is explained by the fact that a large fullerene has a greater number of vibrational degrees of freedom, which are excited during the collision.

For the velocity range $83<V_{C20}<140$ Å/ps, the two fullerenes have energy high enough to overcome the Pauli repulsion, and formation of the new chemical bonds occurs. The center of gravity of the new structure after the collision is at rest and the entire energy of the translational motion of the molecules is spent for creation of the new valence bonds and for excitation of internal oscillations. Bonding of the two fullerenes leads to the appearance of a concave region on C_{540} due to the action of Pauli repulsive forces between them.

High-energy collisions at $V_{C20}>140$ Å/ps, are accompanied by the destruction of one or both fullerenes and formation of new carbon clusters. Collisions of different fullerenes can be observed in detonation chambers during their synthesis or in a mixture of gases of various fullerenes [29,36].

In the present work, a set of regimes for fullerene head-on collisions has been identified, but further details, such as effect of the fullerene size, slash collision, etc. require extensive investigations, which will be pursued in future studies. It is also important

to address the effect of defects on the collision outcomes [50-54]. Such studies are of high importance for understanding the collision behavior and fullerene formation in technological processes.

ACKNOWLEDGEMENTS

The work of R.L.Kh. (creation of the initial structure) was supported by the Russian Science Foundation, grant no. 14-13-00982. The MD simulations were conducted by I.P.L. and J.A.B. (supported by the grant of the President of the Russian Federation for state support of young Russian scientists - doctors of sciences MD-1651.2018.2). The work of S.V.D. (discussion of the results) was supported by the Russian Foundation for Basic Research, grant 17-02-00984-a. This work was also partly supported by the Tomsk State University Competitiveness Improvement Program and IMSP RAS State Assignment. Computational resources were provided by the Federal Agency of Scientific Organizations State Assignment for IMSP RAS.

REFERENCES

[1] H. W. Kroto, J. R. Heath, S. C. O'Brien, R. F. Curl and R. E. Smalley // *Nature* **318** (1985) 162.
[2] J. Coro, M. Suarez, L. S. Silva, K. I. Eguiluz and G. R. Salazar-Banda // *International Journal of Hydrogen Energy* **41** (2016) 17944.
[3] T. Gatti, E. Menna, M. Meneghetti, M. Maggini, A. Petrozza and F. Lamberti // *Nano Energy* **41** (2017) 84.
[4] F. Moussa, *Nanobiomaterials* (Elsevier, Berlin, 2018).
[5] S. Goodarzi, T. D. Ros, J. Conde, F. Sefat and M. Mozafari // *Materials Today* **20** (2017) 460.
[6] M. E. Turan, Y. Sun and Y. Akgul // *Journal of Alloys and Compounds* **740** (2018) 1149.
[7] S. Bronnikov, A. Podshivalov, S. Kostromin, M. Asandulesa and V. Cozan // *Physics Letters A* **381** (2017) 796.
[8] V. V. Shunaev, G. V. Savostyanov, M. M. Slepchenkov and O. E. Glukhova // *RSC Advances* **5** (2015) 86337.
[9] B. Nguyen, A. Cruz, D. McGregor and G. E. Lopez // *Physics Letters A* **381** (2017) 298.
[10] S. Ye, M. Xu, S. FitzGerald, K. Tchernyshyov and Z. Bavcic // *The Journal of Chemical Physics* **138** (2013) 244707.
[11] F. Sebastianelli, M. Xu, Z. Bacvic, R. Lawler and N. J. Turro // *Journal of the American Chemical Society* **132** (2010) 9826.
[12] P. Schwerdtfeger, L. N. Wirz and J. Avery // *Computational Molecular Science* **5** (2014) 96.
[13] R. Taylor and D. R. M. Walton // *Nature* **363** (1993) 685.
[14] N. Zhevago and V. Glebov // *Physics Letters A* **282** (2001) 97.
[15] E. A. Belenkov and V. A. Greshnyakov // *Physics of the Solid State* **58** (2016) 2145.
[16] J. A. Baimova, L. K. Rysaeva and A. I. Rudskoy // *Diamond Relat. Mater.* **81** (2018) 154.
[17] E. A. Belenkov and V. A. Greshnyakov // *Physics of the Solid State* **57** (2015) 2331.
[18] K. A. Krylova, Y. A. Baimova, S. V. Dmitriev and R. R. Mulyukov // *Physics of the Solid State* **58** (2016) 394.
[19] D. S. Lisovenko, Y. A. Baimova, L. K. Rysaeva, V. A. Gorodtsov and S. V. Dmitriev // *Physics of the Solid State* **59** (2017) 820.
[20] J.A. Baimova, L.K. Rysaeva, S.V. Dmitriev, D.S. Lisovenko, V.A. Gorodtsov and D.A. Indeitsev // *Materials Physics and Mechanics* **33** (2017) 1.
[21] D. S. Lisovenko, J. A. Baimova, L. K. Rysaeva, V. A. Gorodtsov, A. I. Rudskoy and S. V. Dmitriev // *Physica Status Solidi (b)* **253** (2016) 1295.
[22] M. N. Regueiro, P. Monceau and J.-L. Hodeau // *Nature* **355** (1992) 237.
[23] S. Adhikari and R. Chowdhury // *Physics Letters A* **375** (2011) 2166.
[24] K. S. Grishakov, K. P. Katin and M. M. Maslov // *Advances in Physical Chemistry* **2016** (2016) 1.
[25] K. P. Katin and M. M. Maslov // *Physica E* **96** (2018) 6.
[26] H. N. Pishkenari and P. G. Ghanbari // *Current Applied Physics* **17** (2017) 72.
[27] A. I. Kharlamov, M. E. Bondarenko and N. V. Kirillova // *Russian Journal of Applied Chemistry* **85** (2012) 233.
[28] T. Ikeda, T. Kamo and M. Danno // *Applied Physics Letters* **67** (1995) 900.
[29] J. W. Martin, G. J. McIntosh, R. Arul, R. N. Oosterbeek, M. Kraft and T. Shnel // *Carbon* **125** (2017) 132.
[30] U. Makhmanov, O. Ismailova, A. Kokhkharov, E. Zakhidov and S. Bakhramov // *Phys. Lett. A* **380** (2016) 2081.
[31] J. Jakowski, S. Irle and K. Morokuma // *Phys. Rev. B* **82** (2010) 125443.

[32] H. Zettergren, H. A. B. Johansson, H. T. Schmidt, J. Jensen, P. Hvelplund, S. Tomita, Y. Wang, F. Martin, M. Alcami, B. Manil, L. Maunoury, B. A. Huber and H. Cederquist // *The Journal of Chemical Physics* **133** (2010) 104301.
[33] S. Hosseini-Hashemi, A. Sepahi-Boroujeni and S. Sepahi-Boroujeni // *Applied Surface Science* **437** (2018) 366.
[34] R. Delaunay, M. Gatchell, A. Mika, A. Domaracka, L. Adoui, H. Zettergren, H. Cederquist, P. Rousseau and B. Huber // *Carbon* **129** (2018) 766.
[35] A. V. Verkhovtsev, A. V. Korol and A. V. Solovyov // *Physical Review A* **88** (2013) 043201.
[36] H. Zettergren and P. Rousseau // *Physical Review Letters* **110** (2013) 185501.
[37] F. Seitz, H. Zettergren, P. Rousseau, Y. Wang, T. Chen, M. Gatchell, J. D. Alexander, M. H. Stockett, J. Rangama, J. Y. Chesnel, M. Capron, J. C. Poully, A. Domaracka, A. M´ ery, S. Maclot, V. Vizcaino, H. T. Schmidt, L. Adoui, M. Alcam´ ý, A. G. G. M. Tielens, F. Martin, B. A. Huber and H. Cederquist // *The Journal of Chemical Physics* **139** (2013) 330.
[38] V. Bernstein and E. Kolodney // *The Journal of Chemical Physics* **145** (2016) 044303.
[39] E. E. B. Campbell, V. Schyja, R. Ehlich and I. V. Hertel // *Physical Review Letters* **70** (1993) 263.
[40] J. Jakowski, S. Irle, B. G. Sumpter and K. Morokuma // *The Journal of Physical Chemistry Letters* **3** (2012) 1536.
[41] J. Handt and R. Schmidt // *Europhysics Letters* **109** (2015) 63001.
[42] O. Knospe and R. Schmidt, *Theory of Atomic and Molecular Clusters* (Springer, Berlin, 1999).
[43] E.E. Campbell, *Fullerene collision reactions* (Kluwer Academic Publishers, 2004).
[44] S. Plimpton // *J. Comp. Phys*. **117** (1995) 1.
[45] S. J. Stuart, A. B. Tutein and J. A. Harrison // *J. Chem. Phys*. **112** (2000) 6472.
[46] J. Wei Feng, H. Ming Ding and Y. Qiang Ma // *Carbon* **90** (2015) 34.
[47] A. I. Melker and M. A. Krupina // *Materials Physics and Mechanics* **34** (2017) 18.
[48] A. I. Melker and M. A. Krupina // *Materials Physics and Mechanics* **34** (2017) 29.
[49] A. I. Melker and M. A. Krupina // *Materials Physics and Mechanics* **34** (2017) 1.
[50] A. Kochnev, I. Ovid'ko, B. Semenov and Ya.A. Sevastyanov // *Reviews on Advanced Materials Science* **48** (2017) 142.
[51] A. Kochnev, I. Ovid'ko, B. Semenov and Y. Sevastyanov // *Reviews on Advanced Materials Science* **50** (2017) 24.
[52] A. Kochnev and I. Ovid'ko // *Materials Physics and Mechanics* **27** (2016) 60.
[53] A. Kochnev, I. Ovid'ko and B. Semenov // *Reviews on Advanced Materials Science* **47** (2016) 79.
[54] A. Kochnev and I. Ovid'ko // *Reviews on Advanced Materials Science* **43** (2015) 89.